24. E. Sato, K. Sato and Y. Tamakawa, "Film-less computed radiography system for high-speed Imaging," *Ann. Rep. Iwate Med. Univ. Lib. Arts & Sci.*, **35**, pp. 13-23, 2000.

Quasi-monochromatic radiography using a high-intensity quasi-x-ray laser generator

Eiichi Sato[a], Yasuomi Hayasi[b], Etsuro Tanaka[c], Hidezo Mori[d], Toshiaki Kawai[e], Tatsumi Usuki[f], Koetsu Sato[f], Haruo Obara[g], Toshio Ichimaru[h], Kazuyoshi Takayama[i], Hideaki Ido[j] and Yoshiharu Tamakawa[k]

[a] Department of Physics, Iwate Medical University, 3-16-1 Honcho-Dori, Morioka 020-0015, Japan
[b] Electrical Engineering, Hachinohe National College of Technology, 16-1 Tamonoki Uwanotai, Hachinohe 039-1104, Japan
[c] Department of Physiology, School of Medicine, Tokai University, Boseidai, Isehara 259-1193, Japan
[d] Department of Cardiac Physiology, National Cardiovascular Center Research Institute, 5-7-1 Fujishiro-dai, Suita, Osaka 565-8565 Japan
[e] Electron Tube Division #2, Hamamatsu Photonics K.K., 314-5 Shimokanzo, Toyooka Village, Iwata-gun 438-0193, Japan
[f] Toreck Inc., Tsunashima Higashi, Kohoku-Ku, Yokohama 223, Japan
[g] Department of Radiological Technology, College of Medical Science, Tohoku University, 1-1 Seiryo-cho, Sendai 980-0872, Japan
[h] Department of Radiological Technology, School of Allied Medical Sciences, Hirosaki University, 66-1 Hon-cho, Hirosaki 036-8564, Japan
[i] Shock Wave Research Center, Institute of Fluid Science, Tohoku University, 1-1 Katahira, Sendai 980-8577, Japan
[j] Department of Applied Physics, Faculty of Engineering, Tohoku Gakuin University, Tagajo 985-0873, Japan
[k] Department of Radiology, Iwate Medical University, 19-1 Uchimaru, Morioka 020-0023, Japan

ABSTRACT

High-intensity quasi-monochromatic x-ray irradiation from the linear plasma target is described. The plasma x-ray generator employs a high-voltage power supply, a low-impedance coaxial transmission line, a high-voltage condenser with a capacity of about 200 nF, a turbo-molecular pump, a thyristor pulse generator as a trigger device, and a flash x-ray tube. The high-voltage main condenser is charged up to 55 kV by the power supply, and the electric charges in the condenser are discharged to the tube after triggering the cathode electrode. The flash x-rays are then produced. The x-ray tube is of a demountable triode that is connected to the turbo molecular pump with a pressure of approximately 1 mPa. As the electron flows from the cathode electrode are roughly converged to the molybdenum target by the electric field in the tube, the plasma x-ray source, which consists of metal ions and electrons, forms by the target evaporating. Both the tube voltage and current displayed damped oscillations, and their peak values increased according to increases in the charging voltage. In the present work, the peak tube voltage was almost equal to the initial charging voltage of the main condenser, and the peak current was about 20 kA with a charging voltage of 55 kV. When the charging voltage was increased, the linear plasma x-ray source formed, and the characteristic x-ray intensities of K-series lines increased. The quasi-monochromatic radiography was performed by a new film-less computed radiography system.

Medical Imaging 2002: Physics of Medical Imaging, Larry E. Antonuk, Martin J. Yaffe, Editors,
Proceedings of SPIE Vol. 4682 (2002) © 2002 SPIE ·1605-7422/02/$15.00

1. INTRODUCTION

The flash x-ray generators produce high-dose-rate x-rays with durations of less than 1 μs, and the x-ray photon energy has been increased up to about 1 MeV[1,2] in the cases where Marx-type high-voltage pulse generators are employed. Next, the energy has been increased up to about 10 MeV[3,4] for the radiography in detonics using an induction-type high-voltage pulse generator. Although the flash x-rays have been generated by the pulse laser, low-prized generators can be realized by the condenser discharging.[5-11]

Recently, we have developed several different plasma flash x-ray generators[12-18] in order to increase the conversion efficiency of the electrostatic energies into x-rays and to generate higher-intensity x-rays. Using these generators, we have found the irradiation of higher-intensity characteristic x-rays by forming the plasma x-ray source using rod and plate targets, because the bremsstrahlung x-rays with energies of higher than K-absorption edge are absorbed by the plasma and are converted into fluorescent and characteristic x-rays. In 2001, we have developed a plasma flash x-ray generator having a new radiation tube[19-21] for forming linear plasma and have performed tentative study on quasi-monochromatic parallel radiography. In the linear plasma, the characteristic x-ray amplification may be performed when the bremsstrahlung rays are absorbed effectively by the linear plasma. In addition, the K-fluorescent yield increases and becomes to one according to increases in the atomic number of target.

In order to form the metal plasma easily, targets with lower melting points are useful, and we have succeeded in generating higher-intensity characteristic x-rays by forming the nickel,[12] copper,[20] silver,[21] and cerium[17] plasmas. In addition, since the radiographic characteristics slightly vary corresponding the target element, we have to measure the characteristics of high-melting-point targets such as tungsten and molybdenum.

For this research, we introduce a flash x-ray generator utilizing a molybdenum-target radiation tube and have performed tentative experiment for generating higher-intensity quasi-monochromatic x-rays by the new amplification method in the characteristic x-rays.

2. GENERATOR

2.1. Setup

Figure 1 shows the block diagram of a high-intensity plasma flash x-ray generator. This generator employs a high-voltage power supply, a high-voltage condenser with a capacity of about 200 nF, a turbo-molecular pump, a thyristor pulse generator as a trigger device, and a flash x-ray tube. In this generator, a low-impedance transmission line is employed in order to increase the maximum tube current. The high-voltage main condenser is charged up to 55 kV by the power supply, and the electric charges in the condenser are discharged to the tube after triggering the cathode electrode. The plasma flash x-rays are then produced.

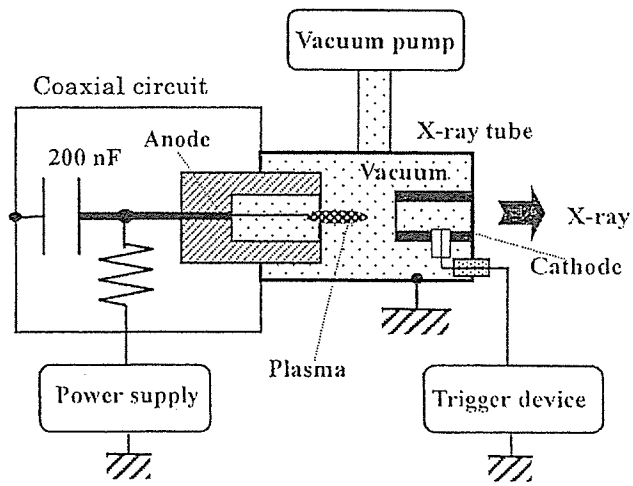

Fig. 1 Block diagram of the high-intensity plasma flash x-ray generator.

2.2 Plasma x-ray tube

The x-ray tube is of a demountable cold-cathode triode that is connected to the turbo molecular pump with a pressure of approximately 1 mPa (Fig. 2). This tube consists of the following major parts: a pipe-shaped carbon cathode with a hole diameter of 10.0 mm, a trigger electrode made from a copper wire, a stainless-steel vacuum chamber, insulators, a polyethylene terephthalate x-ray window of 0.25 mm, and a rod molybdenum target of 3.0 mm in diameter. The space between the anode and cathode electrodes has a value of approximately 15 mm, and the trigger electrode is set in the cathode electrode. As the electron beams from the cathode electrode are roughly converged to the target by the electric field in the tube, the plasma x-ray source, which consists of metal ions and electrons, forms by the target evaporating.

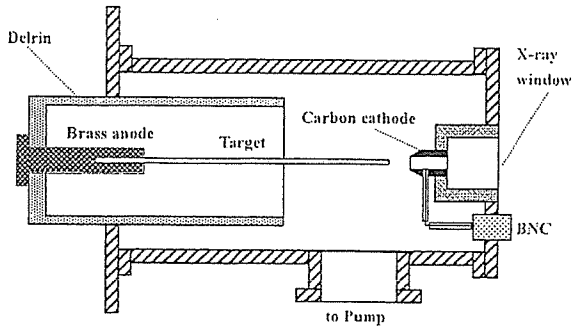

Fig. 2 Schematic drawing of the flash x-ray tube having a rod target.

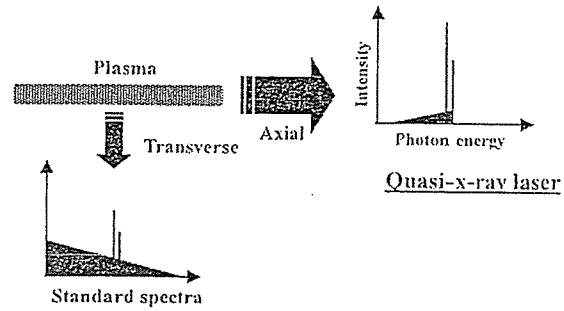

Fig. 3 Principle for generating higher-intensity quasi-monochromatic x-rays.

The principle for generating K-series characteristic x-rays is shown in Fig. 3. If we assume that the plasma thickness has a small value, the spectra from the transverse direction have a standard distribution without considering L-series characteristic x-rays. Next, the bremsstrahlung spectra with photon energies of higher than the K-absorption edge are effectively absorbed and are converted into the fluorescent x-rays, and the high-intensity characteristic x-rays are generated from the plasma-axial direction.

3. CHARACTERISTICS

3.1 Tube voltage and current

The tube voltage and current were measured by a high-voltage divider with an input impedance of 1 GΩ and a current transformer, respectively (Fig. 4). Figure 5 shows the time relation between the tube voltage and current. At the indicated charging voltages, they roughly displayed damped oscillations. When the charging voltage was increased, both the peak tube voltage and current increased. In the present work, the initial tube voltage was almost equal to the initial condenser charging voltage. The maximum tube current was about 20 kA with a charging voltage of 55 kV.

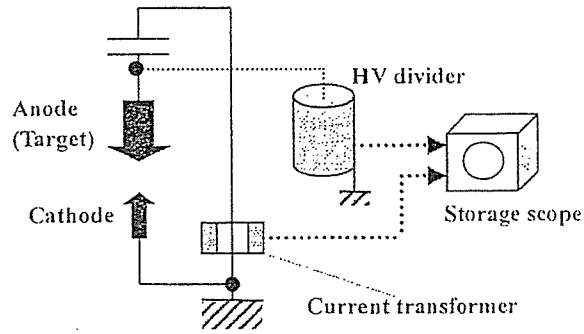

Fig. 4 Methods for measuring the tube voltage and current.

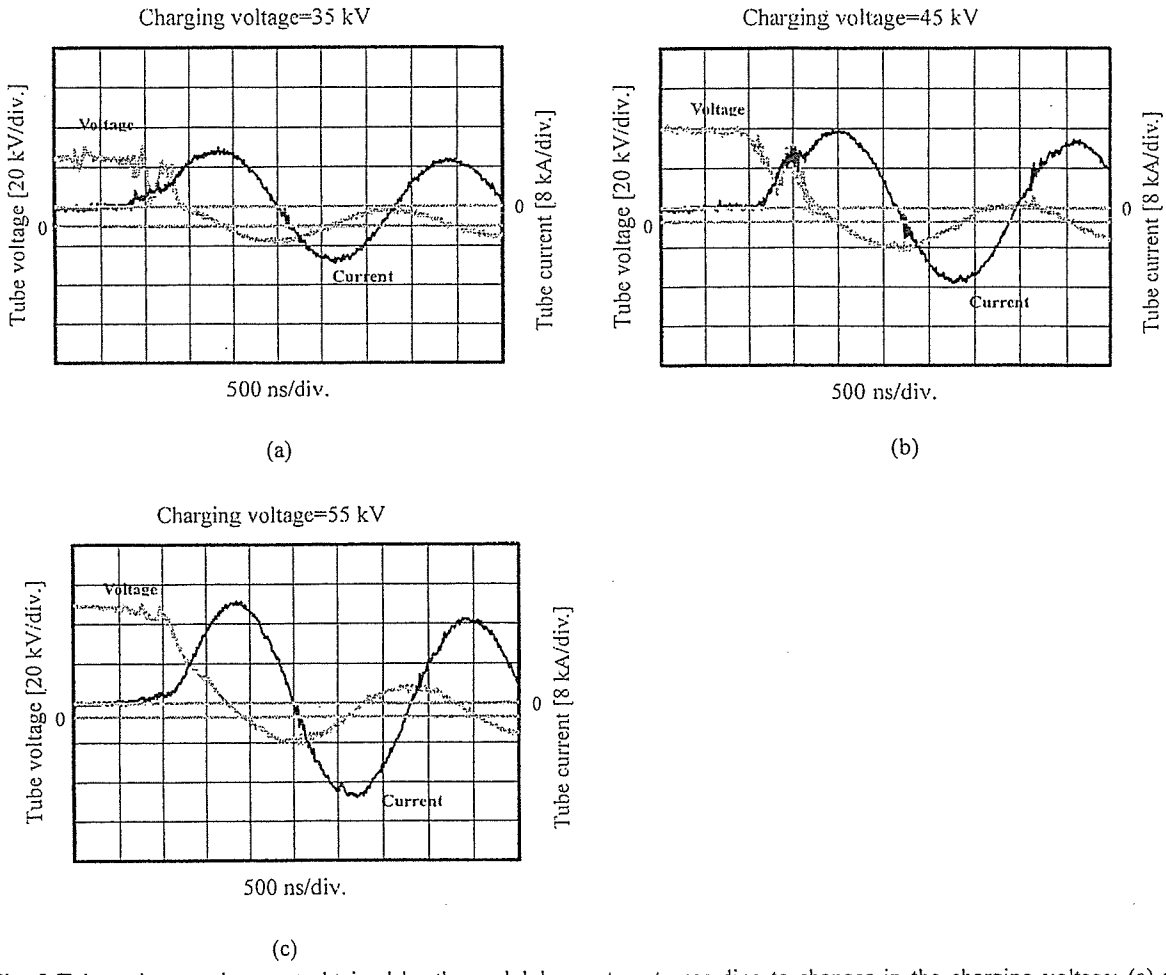

Fig. 5 Tube voltage and current obtained by the molybdenum target according to changes in the charging voltage: (a) with a charging voltage of 35 kV, (b) with a voltage of 45 kV, and (c) with a voltage of 55 kV.

3.2 X-ray output

The x-ray output was detected by using a combination of a plastic scintillator and a photomultiplier (Fig. 6). The x-ray pulse height increased with corresponding increases in the charging voltage and decreased in the case where the monochromatic filter for absorbing bremsstrahlung x-rays was inserted (Fig. 7).

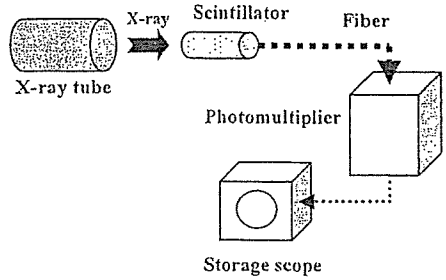

Fig. 6 Method for measuring the x-ray output using a plastic scintillator.

3.3 X-ray source

In order to measure the image of the plasma x-ray source, we employed a pinhole camera with a hole diameter of 100 μm (Fig. 8). When the charging voltage was increased, the plasma x-ray source grew, and the spot intensity increased. In contrast, the intensity decreased according to insertion of the monochromatic molybdenum filter.

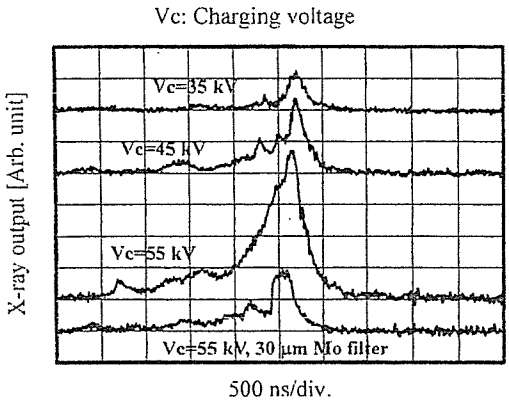

Fig. 7 X-ray outputs at the indicated conditions.

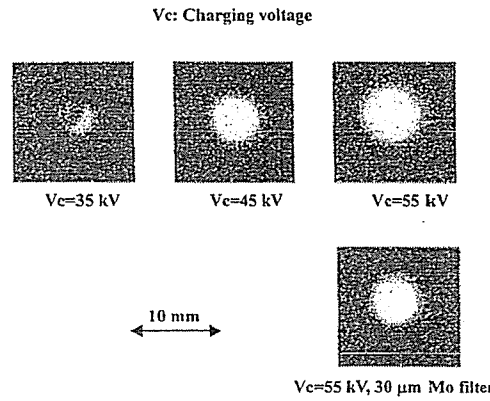

Fig. 8 Images of the plasma x-ray source.

3.4 X-ray spectra

The x-ray spectra from the plasma source were measured by a transmission-type spectrometer having a lithium fluoride curved crystal of 0.5 mm in thickness (Fig. 9). Figure 10 shows the measured spectra from the molybdenum target using an x-ray film (Polaroid XR-7). Spectral intensities of the characteristic x-rays increased with corresponding increases in the charging voltage, and the photon energies corresponded well to the Table 1. According to increases in the shot number, the molybdenum K-series characteristic x-rays and K-absorption edge were clearly observed.

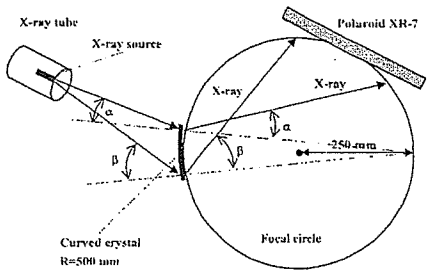

Fig. 9 X-ray spectrometer.

Table 1 Molybdenum K-series characteristic x-rays.

Molybdenum K-Series

	Photon Energy (keV)	Relative Intensity
$K_{\alpha 1}$	17.476	100
$K_{\alpha 2}$	17.371	50
$K_{\alpha 1}$ & $K_{\alpha 2}$	17.441	150
$K_{\beta 1}$	19.605	17
$K_{\beta 3}$	19.587	7

4. RADIOGRAPHY

The radiography was performed by a novel Computed Radiography (CR) system[22] utilizing imaging plates, and the charging voltage and the distance between the x-ray source and the imaging plate were 50 kV and 1.2 m, respectively.

The radiograms of a test chart for measuring the image resolution are shown in Fig. 11. The image resolution is determined by the dimension of the focal spot, the distance between the x-ray source and the imaging plate, and the distance between the radiographic object and the imaging plate, and the resolution had a value of about 100 μm. This resolution is almost equal to one of CR system. Figure 12 shows radiograms of a concentric-circled step of 5.0 mm made of polymethyl methacrylate (PMMA) with a maximum height of 25.0 mm. In this radiography, we obtained almost the same contrast images even when the monochromatic filter was employed or not.

Figure 13 shows angiograms of a heart extracted from a dog using an iodine-based contrast medium, and the fine blood vessel are clearly visible in the enlarged angiogram. Finally, an angiogram of the ear of a rabbit using the same contrast medium is shown in Fig. 14, and fine blood vessels are clearly visible.

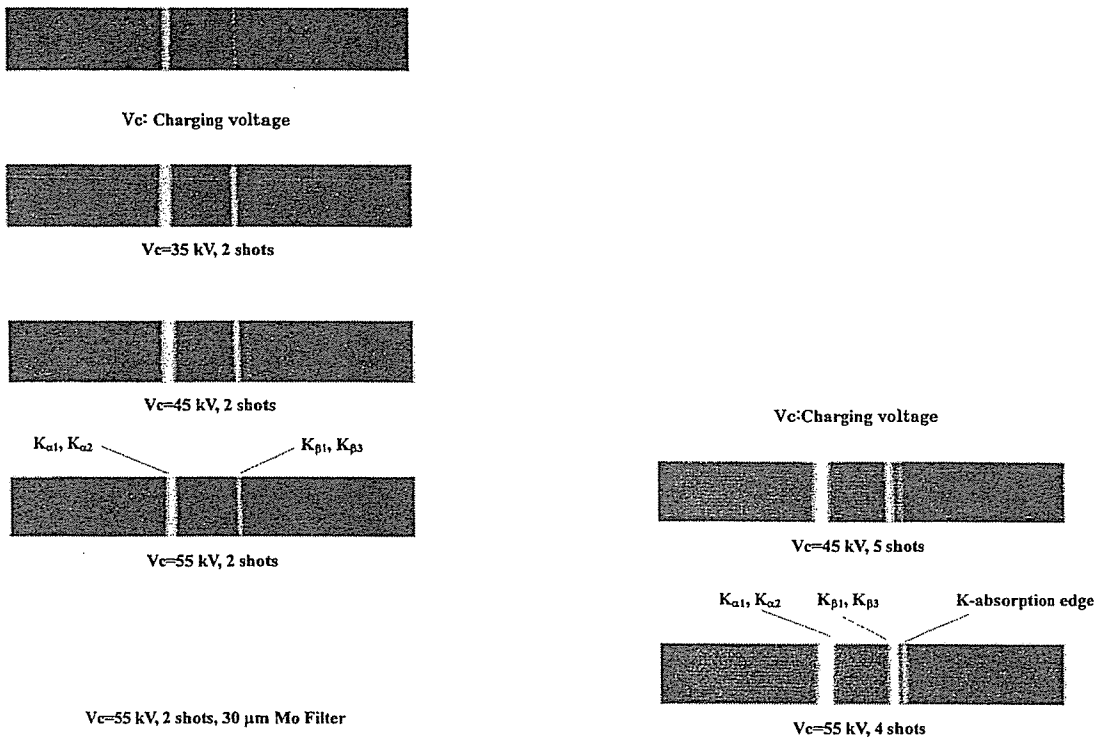

(a) (b)

Fig. 10 X-ray spectra from the molybdenum-plasma target at the indicated conditions:
(a) x-ray spectra by two shots and (b) x-ray spectra by five and four shots.

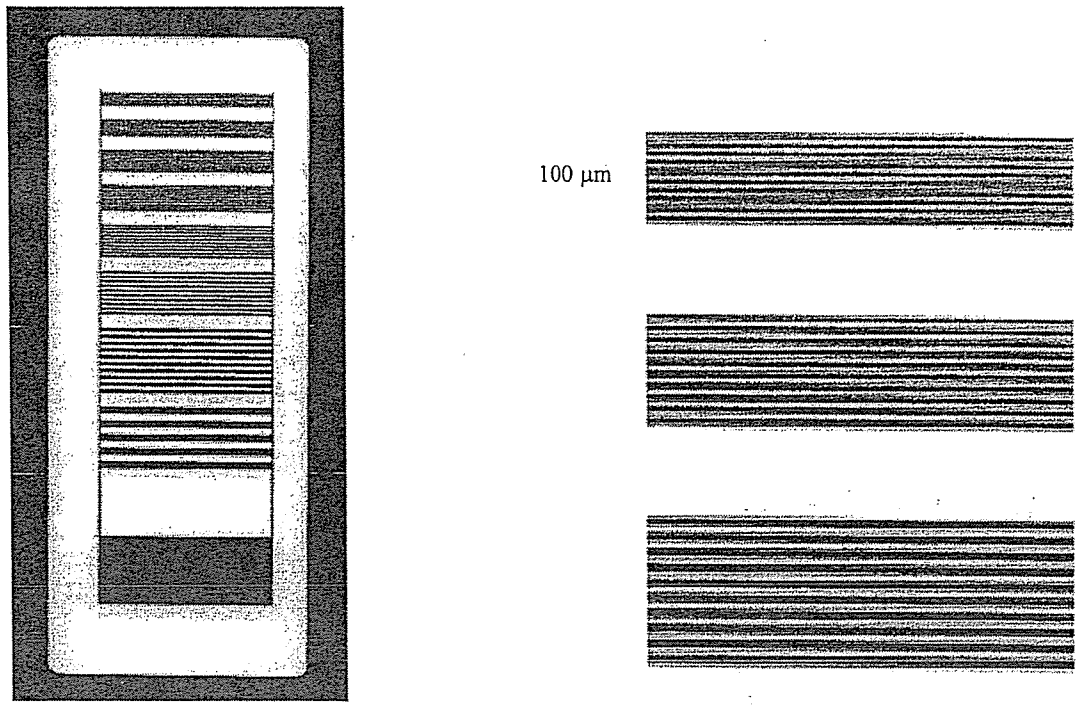

(a) (b)

Fig. 11 Radiograms of a test chart for measuring the image resolution with a charging voltage of 50 kV: (a) normal image and (b) enlarged image.

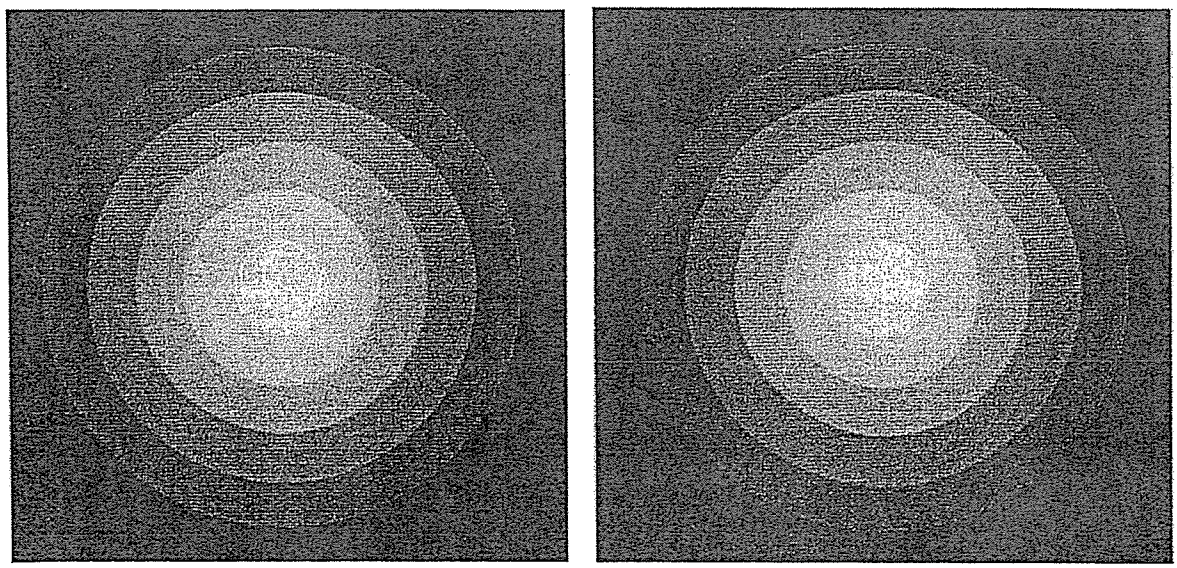

(a) (b)

Fig. 12 Radiograms of a concentric-circled step made of polymethyl methacrylate (PMMA) with a charging voltage of 50 kV: (a) no filter and (b) with a monochromatic molybdenum filter of 30 μm.

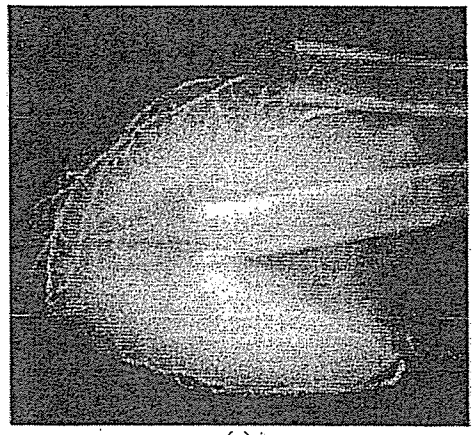

(a)

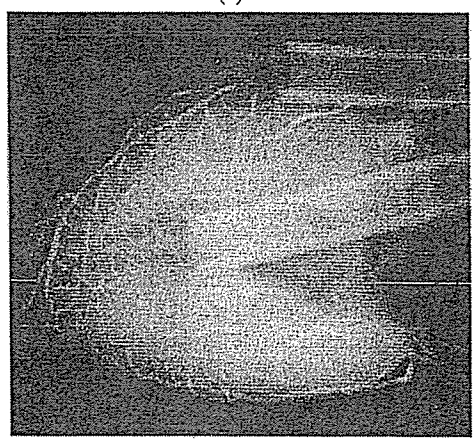

(b)

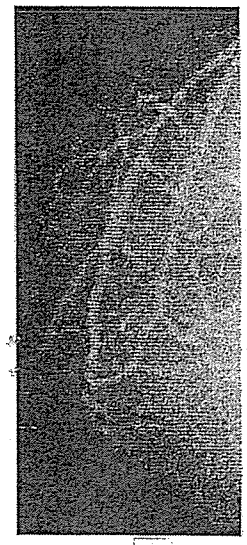

(c)

Fig. 13 Angiogram of a heart extracted from a dog: (a) normal image, (b) enlarged image, and (c) normal image with a molybdenum filter.

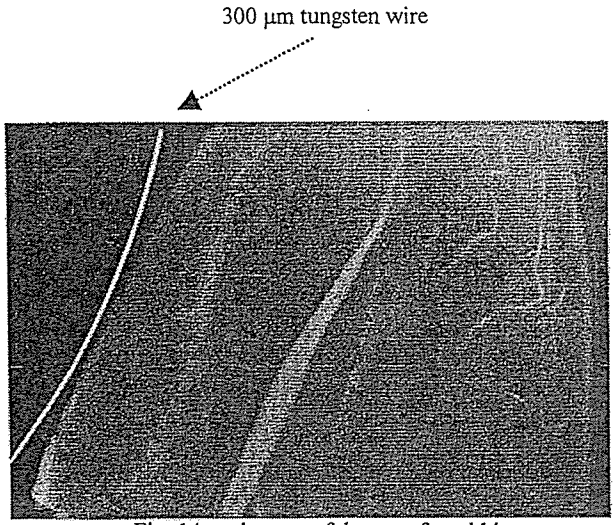

Fig. 14 angiogram of the ear of a rabbit

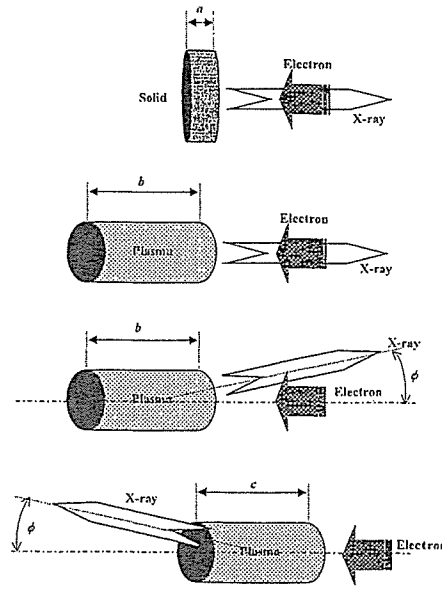

Fig. 15 Solid and plasma targets.

5. DISCUSSION

In the present work, we have succeeded in generating high-intensity characteristic x-rays using the plasma flash x-ray generator having a new radiation tube and have performed high-intensity soft radiography such as manmography. In the spectrum measurement, we observed the K-absorption edges clearly, and bremsstrahlung x-rays were not so detected in the region of higher than the K-edge.

In the cases where the cold-cathode triodes are employed, although there are inductances in the transmission lines, the discharge resistance in the x-ray tube should be increased as large as possible. In these cases, because the high-voltage line is equivalent to the resistor-condenser (RC) series circuit, all the electrostatic energy U in the condenser is consumed by the x-ray tube.

$$U = CV_c^2/2 \cong \int_0^T V(t) \cdot J(t)\, dt, \tag{1}$$

where C is the condenser capacity, V_c is the initial charging voltage, T is the x-ray duration, $V(t)$ is the tube voltage as a function of time t, and $J(t)$ is the tube current. Thus the stable x-ray intensity is obtained by increasing the space between the anode and cathode electrodes in the tube. In this condition, the tube current $J(t)$ and the electrostatic energy U_k for generating K-series characteristic x-rays are written by:

$$J(t) = -C\, d\, V(t) / dt, \tag{2}$$

$$U_k = (V_c^2 - V_k^2)\, C/2, \tag{3}$$

where V_k is the critical excitation voltage of characteristic x-rays.

Figure 15 shows the x-ray generations from the solid and plasma targets. In order to calculate the number of K_i photons N_{ki} from the thick target, if we assume that the tube voltage is a constant and is corresponding to the maximum photon energy E_0 to simplify an equation, the photon number N_{ki} [23] is represented by:

$$N_{ki} = K_1\, \omega_k \int_0^a \int_{Ek}^{E_0} N_e(E,x) \cdot \sigma_K(E) \cdot \exp(-\mu_{ki} \cdot x)\, dE\, dx, \tag{4}$$

where ω_k is the K-fluorescent yield, a is the target thickness, μ_{ki} is the linear absorption coefficient of the target, $\sigma_K(E)$ is the cross section for K-photon radiation as a function of photon energy E, $N_e(E,x)$ is the electron distribution at the depth x in the target, E_k is the critical excitation energy, and K_1 is a constant. Therefore, in order to simplify the equation, if we assume that the rod target in the plasma is negligible, the photon number N_{kip} from the plasma may be written by:

$$N_{kip} \cong K_2\, \omega_k \int_0^b \int_{Ek}^{E0} N'_e(E,\xi) \cdot \sigma'_K(E) \cdot \exp(-\mu_{pki} \cdot \xi)\, dE \quad d\xi, \tag{5}$$

$$\mu_{pki} = \mu_{mki} \cdot \rho_e, \tag{6}$$

where b is the plasma length, ξ is the depth, μ_{mki} is the mass absorption coefficient, ρ_e is the effective density of the plasma, and K_2 is a constant. Next, the number varies according to changes in the irradiation angle ϕ and is written by:

$$N_{kip} \cong K_2\, \omega_k \int_0^b \int_{Ek}^{E0} N'_e(E,\xi) \cdot \sigma'_K(E) \cdot \exp(-\mu_{pki} \cdot \xi \cdot \sec\phi)\, dE \quad d\xi. \tag{7}$$

Thus, in the transmission-type plasma with a length c, the number is represented by:

$$N_{kip} \cong K_2\, \omega_k \int_0^c \int_{Ek}^{E0} N'_e(E,\xi) \cdot \sigma'_K(E) \cdot \exp\{-\mu_{pki} \cdot (c-\xi) \cdot \sec\phi\}\, dE \quad d\xi. \tag{8}$$

Compared with the target such as silver with a lower melting temperature, it is difficult to form molybdenum plasma x-ray source at a lower charging voltage of about 40 kV. In view of this situation, the current density at the target tip should be increased as large as possible by increasing the condenser capacity and by decreasing the target diameter.

ACKOWLEDGEMENTS

This work was supported by Grants-in-Aid for Scientific Research (12670902, 13470154 and 13877114) from MECSST, Japan Science and Technology Corporation, Scientific Research from New Energy and Industrial Technology Development Organization, and Cardiovascular Disease (H13C-1) from MHLW.

REFERENCES

1. A. Mattsson, "Some characteristics of a 600 kV flash x-ray tube," *Physica Scripta*, **5**, pp. 99-102, 1972.

2. R. Germer, "X-ray flash techniques," *J. Phys. E: Sci. Instrum.*, **12**, pp. 336-350, 1979.

3. C. Cavailler, "AIRIX: an induction accelerator facility developed at CEA for flash radiography in detonics," *SPIE*, **3516**, pp. 25-35, 1998.

4. C. Cavailler, "AIRIX- a new tool for flash radiography in detonics," *SPIE*, **4183**, pp. 23-35, 2000.

5. E. Sato, S. Kimura, S. Kawasaki, H. Isobe, K. Takahashi, Y. Tamakawa and T. Yanagisawa, "Repetitive flash x-ray generator utilizing a simple diode with a new type of energy-selective function," *Rev. Sci. Instrum.*, **61**, pp. 2343-2348, 1990.

6. E. Sato, M. Sagae, K. Takahashi, T. Oizumi, H. Ojima, K. Takayama, Y. Tamakawa, T. Yanagisawa, A. Fujiwara and K. Mitoya, "High-speed soft x-ray generators in biomedicine," *SPIE*, **2513**, pp. 649-667, 1994.

7. A. Shikoda, E. Sato, M. Sagae, T. Oizumi, Y. Tamakawa and T. Yanagisawa, "Repetitive flash x-ray generator having a high-durability diode driven by a two-cable-type line pulser," *Rev. Sci. Instrum.*, **65**, pp. 850-856, 1994.

8. E. Sato, K. Takahashi, M. Sagae, S. Kimura, T. Oizumi, Y. Hayasi, Y. Tamakawa and T. Yanagisawa, "Sub-kilohertz flash x-ray generator utilizing a glass-enclosed cold-cathode triode," *Med. & Biol. Eng. & Comput.*, **32**, pp. 289-294, 1994.

9. K. Takahashi, E. Sato, M. Sagae, T. Oizumi, Y. Tamakawa and T. Yanagisawa, "Fundamental study on a long-duration flash x-ray generator with a surface-discharge triode," *Jpn. J. Appl. Phys.*, **33**, pp. 4146-4151, 1994.

10. E. Sato, M. Sagae, A. Shikoda, K. Takahashi, T. Oizumi, M. Yamamoto, A. Takabe, K. Sakamaki, Y. Hayasi, H. Ojima, K. Takayama and Y. Tamakawa, "High-speed soft x-ray techniques, " *SPIE*, **2869**, pp. 937-955, 1996.

11. E. Sato, M. Sagae, K. Sakamaki and Y. Tamakawa, "Tentative experiment for generating x-rays from the vacuum space," *Ann. Rep. Iwate Med. Univ. Sch. Lib. Arts Sci.*, **32**, pp. 11-18, 1997.

12. E. Sato, M. Sagae, K. Takahashi, K. Sakamaki and Y. Tamakawa, "Quasi-monochromatic nickel-plasma radiography," *Ann. Rep. Iwate Med. Univ. Sch. Lib. Arts Sci.*, **32**, pp. 1-10, 1997.

13. E. Sato, M. Sagae, K. Takahashi, T. Ichimaru, A. Wataru, S. Kumagai, H. Ido, K. Sakamaki, K. Takayama and Y. Tamakawa, "Monochromatic plasma x-ray generator and its applications," *SPIE*, **3336**, pp. 75-86, 1998.

14. E. Sato, M. Sagae, T. Ichimaru, K. Takahashi, H. Ojima, K. Takayama, Y. Hayasi, H. Ido, K. Sakamaki and Y. Tamakawa, "Characteristics of the plasma flash x-ray generator and applications," *SPIE*, **3516**, pp. 626-635, 1998.

15. K. Takahashi, E. Sato, M. Sagae and Y. Tsukahara, "Semi-monochromatic plasma flash radiography and its application to biomedical image simulation," *Jpn. J. Appl. Phys.*, **37**, pp. 4222-4227, 1998.

16. E. Sato, M. Sagae, T. Ichimaru, Y. Hayasi, H. Ojima, K. Takayama, H. Ido, K. Sakamaki and Y. Tamakawa, "Tentative study on x-ray enhancement by fluorescent emission of radiation by plasma x-ray source," *SPIE*, **3771**, pp. 51-60, 1999.

17. E. Sato, Y. Hayasi, H. Mori, E. Tanaka, K. Takayama, H. Ido, K. Sakamaki and Y. Tamakawa, "Quasi-monochromatic x-ray production from the cerium target," *SPIE*, **4142**, pp. 17-28, 2000.

18. E. Sato, Y. Hayasi, T. Ichimaru, H. Mori, E. Tanaka, H. Ojima, K. Takayama, T. Usuki, K. Sato, K. Sakamaki and Y. Tamakawa, "Tentative study on high-photon-energy quasi-x-ray laser generator by forming plasma x-ray source," *SPIE*, **4183**, pp. 326-338, 2000.

19. E. Sato, Y. Suzuki, Y. Hayashi, E. Tanaka, H. Mori, T. Kawai, K. Takayama, H. Ido and Y. Tamakawa, "High-intensity quasi-monochromatic x-ray irradiation from the linear plasma target," *SPIE*, **4505**, pp. 154-164, 2001.

20. E. Sato, Y. Hayasi, E. Tanaka, H. Mori, T. Kawai, H. Obara, T. Ichimaru, K. Takayama, H. Ido, T. Usuki, K. Sato and Y. Tamakawa, "Polycapillary radiography using a quasi-x-ray laser generator," *SPIE*, **4508**, pp. 176-187. 2001.

21. E. Sato, Y. Hayasi, H. Ojima, K. Takayama and Y. Tamakawa, "High photon energy quasi-x-ray laser generator for shock wave research," *Proc. 23rd Symp. on Shock Waves, Fort Worth*, 2001, to be published.

22. E. Sato , Y. Hayasi and Y. Tamakawa, "Film-less computed radiography system for high-speed Imaging," *Ann. Rep. Iwate Med. Univ. Lib. Arts and Sci.*, **35**, pp. 13-23, 2000.

23. N. Nakamori, K. Yamano, M. Yamada and H. Kanamori, "Calculation of characteristic x-rays in diagnostic x-ray spectrum," *Jpn. J. Appl. Phys.*, **33**, pp. 347-352, 1994.

Annual Report of Iwate Medical University
School of Liberal Arts and Sciences
No. 37(2002), 23-32.

Quasi-monochromatic parallel radiography achieved with a plane-focus x-ray tube

Eiichi Sato[a], Yasuomi Hayasi[b], Etsuro Tanaka[c], Hidezo Mori[d], Makoto Komatsu[e], Haruo Obara[e], Toshio Ichimaru[f] and Kazuyoshi Takayama[g]

(Received October 18, 2002)

ABSTRACT

Fundamental study on quasi-monochromatic parallel radiography using a polycapillary plate and a plane-focus x-ray tube is described. The x-ray generator consists of a negative high-voltage power supply, a filament (hot cathode) power supply, and an x-ray tube. The negative high-voltage is applied to the cathode electrode, and the transmission type target (anode) is connected to the ground potential. In this experiment, the tube voltage was regulated from 20 to 25 kV, and the tube current was regulated by the filament temperature and ranged from 1.0 to 3.0 mA. The exposure time was controlled in order to obtain optimum film density, and the focal spot diameter was about 10 mm. The polycapillary plate is J5022-21 made by Hamamatsu Photonics Inc. with a plate thickness of 1.0 mm. The outer, effective, and hole diameters are 87 mm, 77 mm, and 25 μm, respectively. The x-rays from the tube are formed into parallel beam by the polycapillary, and the radiogram is taken using an industrial x-ray film of Fuji IX 100 without using a screen. In the measurement of image resolution, we employed three brass spacers of 2, 30, and 60 mm in height. By the test chart, the resolution fell according to increases in the spacer height without using a polycapillary. In contrast, the resolution slightly fell with corresponding increases in the height by the polycapillary. In angiography, fine blood vessels of about 100 μm are clearly visible.

1. INTRODUCTION

Synchrotrons generate high dose rate bremsstrahlung x-rays, and monochromatic parallel radiography has been performed using silicon monochromators. These radiations play important roles in

[a] Department of Physics, Iwate Medical University, 3-16-1 Honchodori, Morioka 020-0015, Japan
[b] Electrical Engineering, Hachinohe National College of Technology, 16-1 Tamonoki Uwanotai, Hachinohe 039-1104, Japan
[c] Department of Physiology, School of Medicine, Tokai University, Boseidai, Isehara 259-1193, Japan
[d] Department of Cardiac Physiology, National Cardiovascular Center Research Institute, 5-7-1 Fujishirodai, Suita, Osaka 565-8565 Japan
[e] Department of Radiological Technology, College of Medical Science, Tohoku University, 1-1 Seiryocho, Sendai 980-0872, Japan
[f] Department of Radiological Technology, School of Health Sciences, Hirosaki University, 66-1 Honcho, Hirosaki 036-8564, Japan
[g] Shock Wave Research Center, Institute of Fluid Science, Tohoku University, 2-1-1 Katahira, Sendai 980-8577, Japan

microangiography[1] and phase-contrast radiography,[2-4] and we tend to long for further applications for a long time. In order to drive a synchrotron, large electric power is needed. Furthermore, it is very difficult to obtain sufficient machine times for various researches.

Thus far, we have developed several different soft flash x-ray generators[5-12] in order to perform soft radiographies including biomedical applications. In particular, plasma flash x-ray generators[13-15] are quite useful to produce higher dose rate quasi-monochromatic x-rays as compared with a synchrotron. When the weakly ionized linear plasma forms using a fine rod target by the high energy discharge, we have found irradiations of quite intense and sharp characteristic x-rays, and these rays have distinctive characteristics such as divergence by slits.

When we employ an parallel x-ray system made by Rigaku Inc. utilizing a line-focus x-ray tube and a reflector, the irradiation field has dimensions of 10×10 mm, and this x-ray system is very expensive. In view of this situation, although several different x-ray lenses[16,17] have been developed, a polycapillary plate[18-20] is useful to realize a low-priced x-ray system and to perform parallel radiography. Using a conventional x-ray generator having a tungsten target radiation tube, we have performed parallel radiography[19] and have obtained image resolutions of about 50 μm or less. However, because the tube has a small focal spot, the irradiation field is very small. In order to increase the field using a polycapillary plate, the spot dimension should be increased as large as possible.

In the present work, we have performed tentative study on quasi-monochromatic parallel radiography utilizing a polycapillary plate and a transmission-type plane-focus x-ray tube in order to create a new x-ray system instead of the synchrotron.

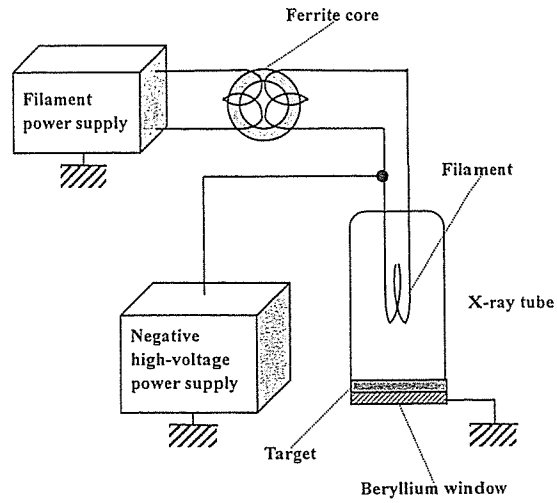

Fig. 1: Circuit diagram of the x-ray generator.

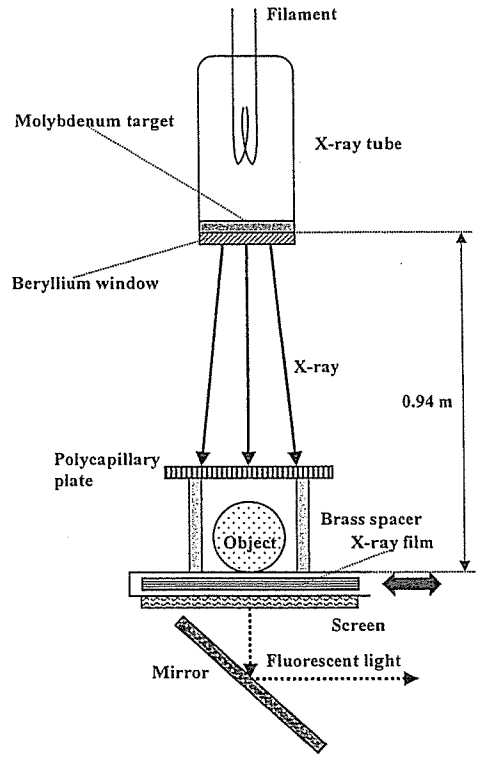

Fig. 2: Experimental setup for parallel radiography.

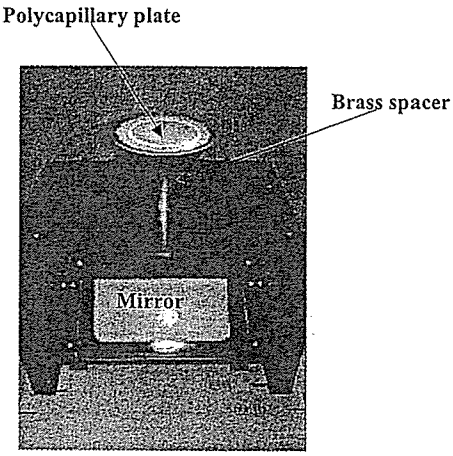

Fig. 3: Inner side of the x-ray generator.

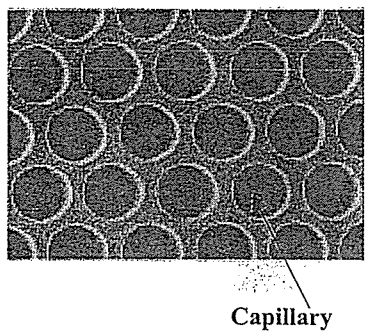

Fig. 4: Magnification of a polycapillary plate.

2. SETUP

The circuit diagram of an x-ray generator is illustrated in Fig. 1, and this generator consists of a negative high-voltage power supply, a filament power supply, and an x-ray tube. The negative high-voltage is applied to the cathode electrode, and the transmission type target (anode) is connected to the ground potential. In this experiment, the tube voltage was regulated from 20 to 25 kV, and the tube current was regulated by the filament temperature and ranged from 1.0 to 3.0 mA. The exposure time is controlled in order to obtain optimum film density, and the focal spot diameter was about 10 mm.

The experimental setup is shown in Figs. 2 and 3, and the quasi-monochromatic x-rays from the plane-focus x-ray tube are formed into parallel beam by the polycapillary. The polycapillary plate is J5022-21 made by Hamamatsu Photonics Inc., and the plate thickness was 1.0 mm. The outer, effective, and hole diameters are 87 mm, 77 mm, and 25 μm, respectively (Fig. 4).

Radiography was performed using an x-ray film (Fuji IX 100), and the x-ray tube employs a transmission type molybdenum target of 25 μm in thickness and a beryllium window.

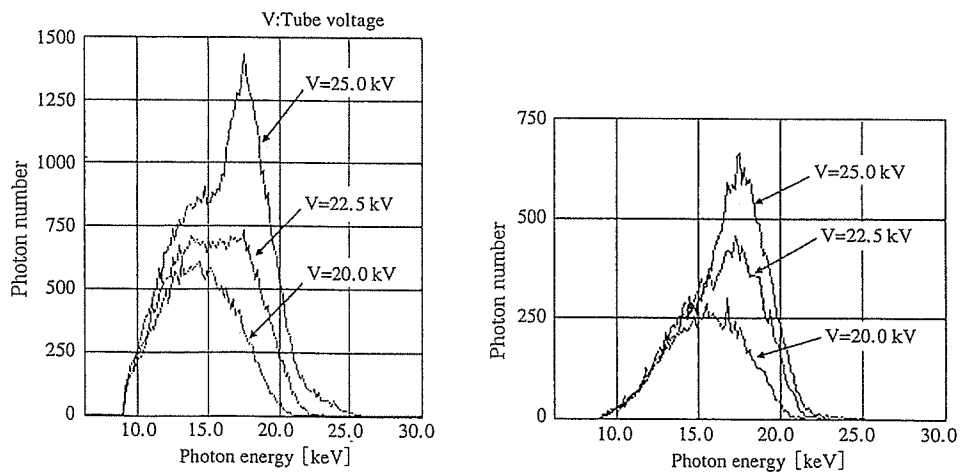

Fig. 5: Measured x-ray spectra according to changes in the tube voltage.

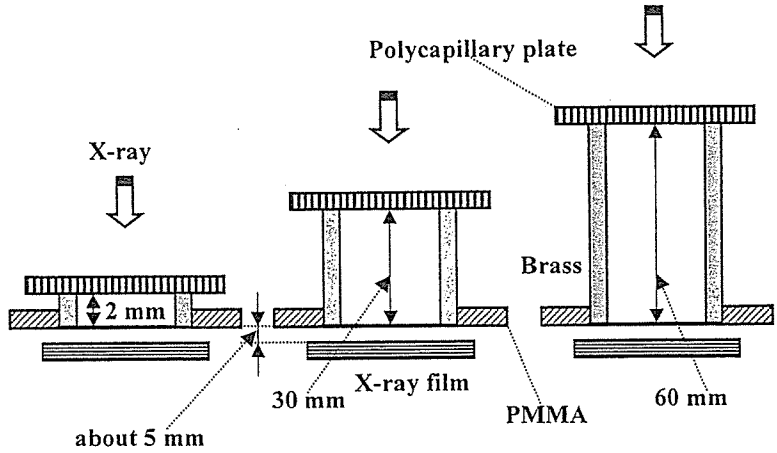

Fig. 6: Radiography for imaging a polycapillary plate.

The distance between the x-ray focus and film is 0.94 m, and the polycapillary plate is placed on the brass spacer, and the radiogram is roughly observed by a setup of screen and mirror.

3. X-RAY SPECTRA

In order to measure x-ray spectra, we employed a cadmium tellurium detector of CDTE2020X made by Hamamatsu Photonics Inc. (Fig. 5). Compared to a germanium detector, this detector has lower energy resolutions, and the characteristic x-ray intensity increased with corresponding increases in the tube voltage at a constant tube current of 1.0 mA. Next, the energy width decreased by the insertion of a 30 μm molybdenum filter.

4. RADIOGRAPHY

The quasi-monochromatic radiography was performed with a charging voltage of 22.5 kV. Figure 6 shows radiography for imaging a polycapillary plate, and the radiograms of the polycapillary are shown in Fig. 7. The center of black spot in the polycapillary radiogram is almost imaged by direct transmission

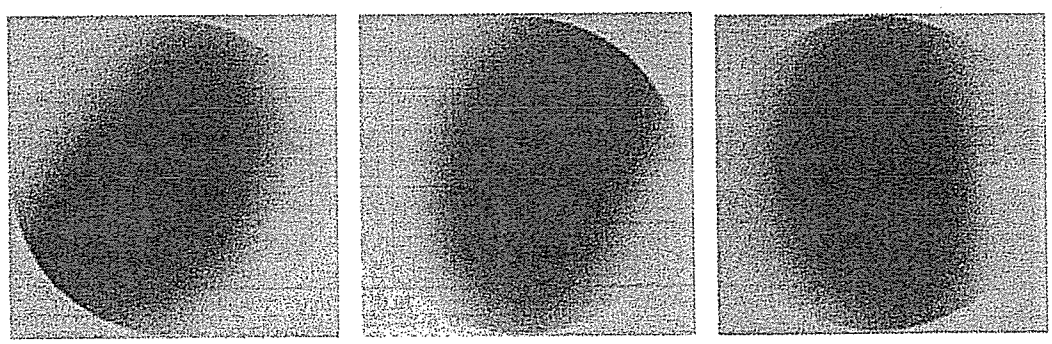

Fig. 7: Radiograms of a polycapillary plate according to changes in the height of brass spacer: (a) 2 mm, (b) 30 mm, and (c) 60 mm.

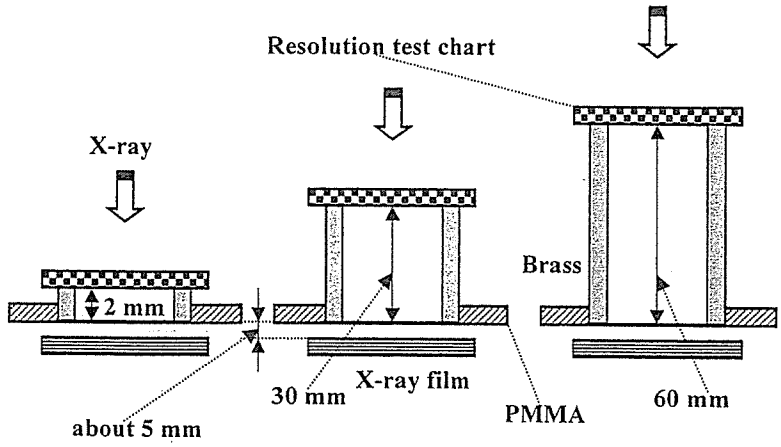

Fig. 8: Radiography for imaging a resolution-test chart.

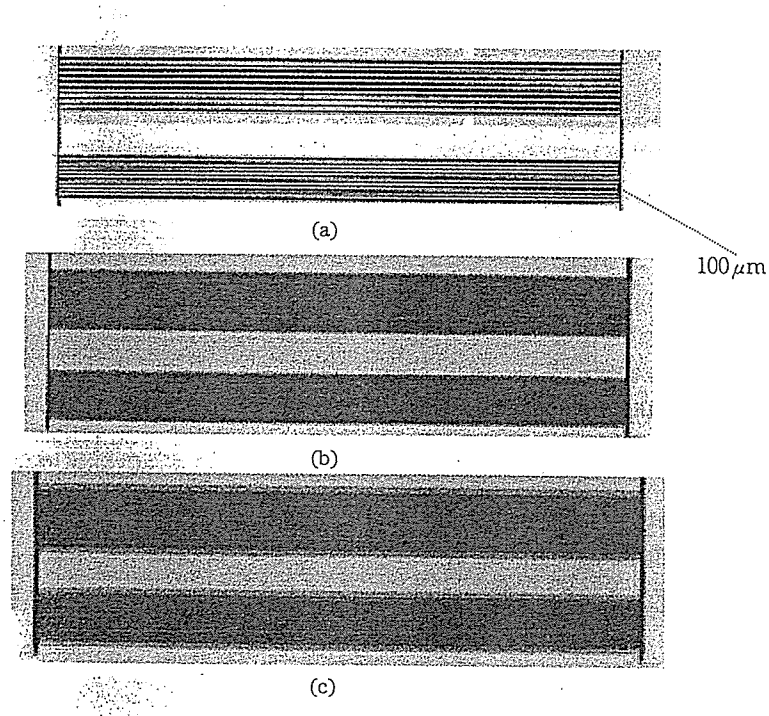

Fig. 9: Radiograms of a test chart according to changes in the brass spacer height : (a) 2 mm, (b) 30 mm, and (c) 60 mm.

beams through capillary holes. As shown in this figure, both the spot density and the dimension seldom varied according to increases in the brass-spacer height.

In order to image a test chart, we employed a setup shown in Fig. 8. Of course, the image resolution improved according to decreases in the spacer height, and we could observe 100 μm lines clearly with a height of 2 mm (Fig. 9). Figure 10 shows the parallel radiography for imaging a test chart, and the

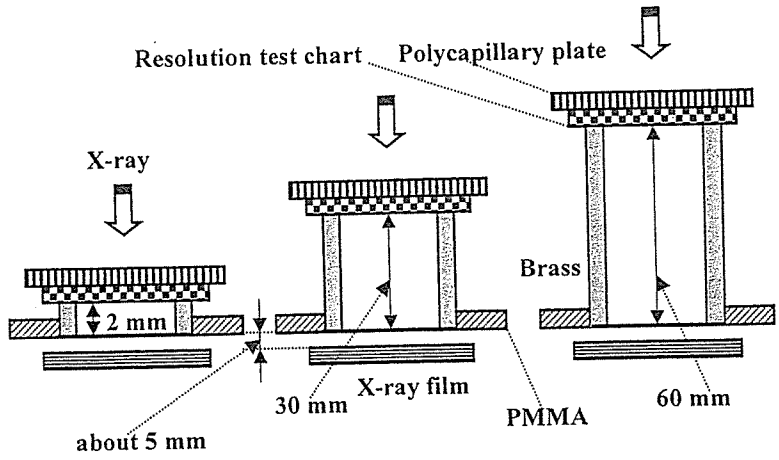

Fig. 10: Radiography for imaging a test chart using a polycapillary plate.

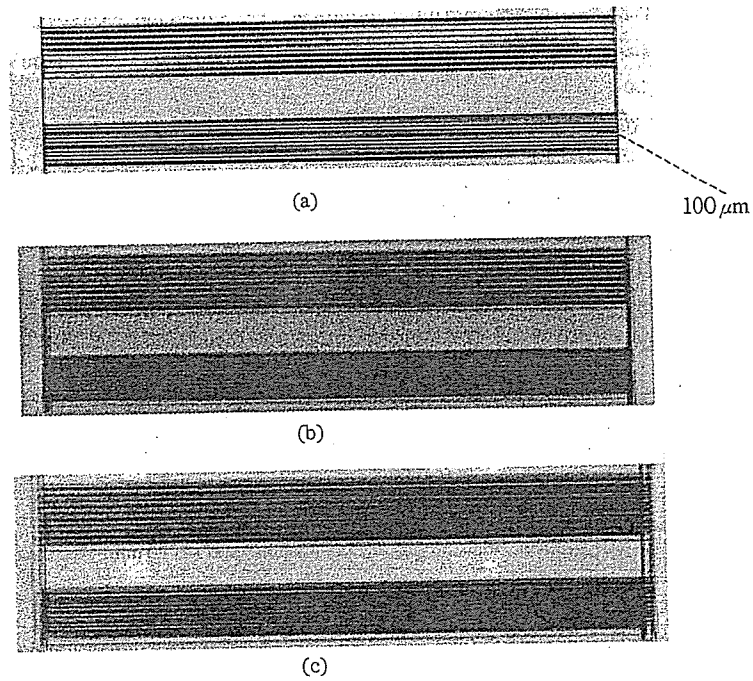

Fig. 11: Radiograms of a test chart according to changes in the brass spacer height using a polycapillary plate: (a) 2 mm, (b) 30 mm, and (c) 60 mm.

polycapillary was placed on the chart. In this radiography, we observed 100 μm lines even when a higher spacer of 30 mm was employed (Fig. 11).

Fig. 12 shows angiograms of a heart extracted from a rabbit using iodine-based microspheres. When the polycapillary is employed with a spacer height of 22 mm, fine blood vessels of about 100 μm are clearly visible.

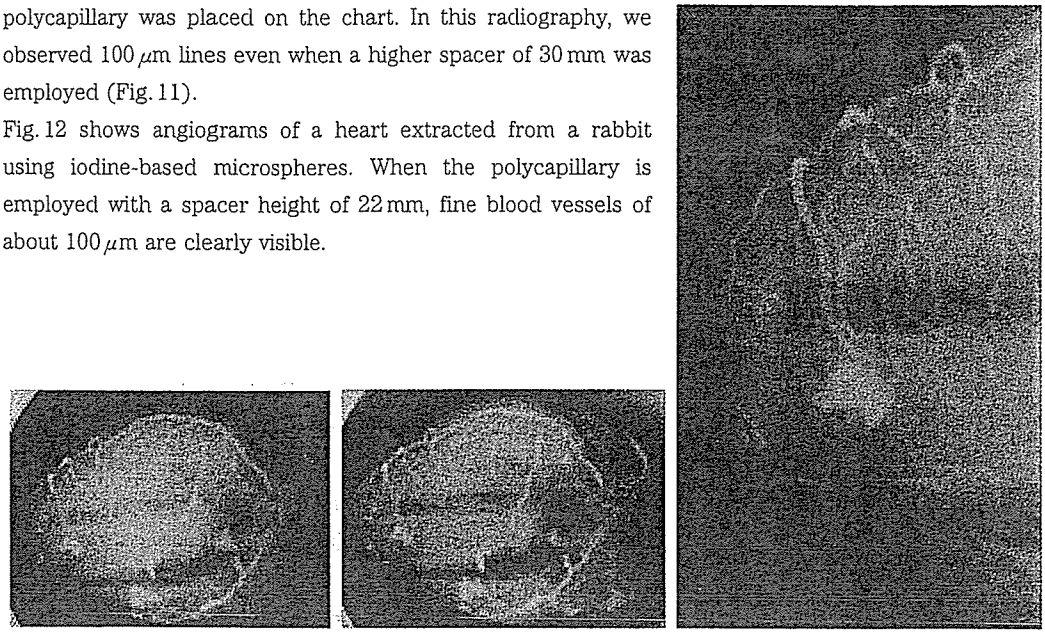

(a) (b) (c)

Fig. 12: Angiograms of a heart extracted from a rabbit using iodine-based micro spheres with a charging voltage of 22.5 kV: (a) without using a polycapillary, (b) using a polycapillary and a 22 mm spacer, and (c) enlarged radiogram using a polycapillary.

5. DISCUSSION

Using this polycapillary, we have obtained higher image resolutions and contrasts, and the resolution improves with corresponding decreases in the capillary diameter. In the spectrum measurement, although molybdenum characteristic x-rays were observed with tube voltages of higher than 22.5 kV, we have to employ germanium detector to increase energy resolution.

In order to calculate the number of K_i photons N_{ki} from the thick target, if we assume that the tube voltage is constant and is corresponding to the maximum photon energy E_0 to simplify an equation, the photon number N_{ki}[27] is represented by:

$$N_{ki} \cong K_1 \, \omega_k \int_0^a \int_{E_k}^{E_0} N_e(E, x) \cdot \sigma_k(E) \cdot \exp\{-\mu_m(E_i)(a - x)\} \, dE \, dx, \tag{1}$$

where ω_k is the K-fluorescent yield, a is the target thickness, $\mu_m(E_i)$ is the linear absorption coefficient of target, $\sigma_k(E)$ is the cross section for K-photon radiation as a function of photon energy E, $N_e(E,x)$ is the electron distribution at the depth x in the target, E_k is the critical excitation energy, and K_1 is a constant.

Currently, we assume that x-rays are produced at the target surface in order to simplify an equation, the characteristic x-ray intensities after transmitting the target I_{ki} is represented by:

$$I_{kt} = \sum_{i=1}^{n} I_k(E_i) \cdot \exp\{-\mu_m(E_i) \cdot a\}, \quad (2)$$

where $I_k(E_i)$ is the characteristic x-ray intensity generated by the target surface.

We assume that the incident angle for reflection in the capillary hole is constant, because the reflecting intensity is approximated, the x-ray intensity without absorbing I_0, the transmission intensity I_t, the reflecting intensity I_r, and the intensity for parallel radiography I may be given by:

$$I_0 = k_2 \cdot I_{kt}, \quad (3)$$

$$I_t \cong k_3 \sum_{i=1}^{n} I_k(E_i) \cdot \exp\{-\mu_m(E_i) \cdot a - \mu_c(E_i) \cdot b\}, \quad (4)$$

$$I_r \cong k_4 \sum_{i=1}^{n} I_k(E_i) \cdot \exp\{-\mu_m(E_i) \cdot a\} \cdot R(E_i)^n, \quad (5)$$

$$I \cong I_0 + I_r >> I_t, \quad (6)$$

where $\mu_c(E_i)$ is the linear absorption coefficient of capillary glass, $R(E_i)$ is the reflecting power ($1 \geqq R(E_i) \geqq 0$), b is the capillary thickness, and $K_2 \sim K_4$ are constants.

For this research, we have performed parallel radiography achieved with a polycapillary plate in conjunction with a quasi-monochromatic x-ray tube and have obtained higher image resolutions as compared with those obtained without using the plate. In the cases where the high photon energy x-rays of higher than 20 keV are employed, the polycapillary thickness should be increased in order to improve the image sharpness by decreasing the transmission intensity.

Using this radiography, because it is possible to improve the image resolution and to employ quasi-monochromatic x-rays, this system can be applied to image a wide variety of objects in various fields including medical radiography.

ACKOWLEDGEMENTS

This work was supported by Grants-in-Aid for Scientific Research (12670902, 13470154 and 13877114) from MECSST, Test of Fostering Potential of Japan Science and Technology Corporation, Scientific Research from New Energy and Industrial Technology Development Organization, and Cardiovascular Disease (H13C-1) from MHLW.

REFERENCES

1. H. Mori, K. Hyodo, E. Tanaka, M.U. Mohammed, A. Yamakawa, Y. Shinozaki, H. Nakazawa, Y. Tanaka, T. Sekka, Y. Iwata, S. Honda, K. Umetani, H. Ueki, T. Yokoyama, K. Tanioka, M. Kubota, H. Hosaka, N. Ishizawa and M. Ando, "Small-vessel radiography in situ with monochromatic synchrotoron radiation," *Radiology*, **201**, pp. 173-177, 1996.
2. T.J. Davis, D. Gao, T.E. Gureyev, A.W. Stevenson and S.W. Wilkims, "Phase-contrast imagimg of weakly absorbing materials using hard x-rays," *Nature*, **373**, pp. 595-597, 1995.
3. A. Momose, T. Takeda, Y. Itai and K. Hirano, "Phase-contrast x-ray computed tomography for observing biological soft tissues," *Nature Medicine*, **2(4)**, pp. 473-475, 1996.
4. A. Ishisaka, H. Ohara and C. Honda, "A new method of analyzing edge effect in phase contrast